EUROPEAN ORGANIZATION FOR NUCLEAR RESEARCH

DIRAC Note 2015-04
September 20, 2015

The estimation of production rates of π^+K^-, π^-K^+ and $\pi^+\pi^-$ atoms in proton-Ni interactions at proton momentum of 450 GeV/c.

O.Gorchakov, L.Nemenov

GENEVA
2015

Abstract

In the DIRAC experiment at CERN the π^+K^-, $K^+\pi^-$ and $\pi^+\pi^-$ atoms generated in proton-nucleus interaction at proton momentum $P_p = 24$ GeV/c were investigated. This work shows that the yields of π^+K^-, $K^+\pi^-$ and $\pi^+\pi^-$ atoms in the p-nucleus interactions at $P_p = 450$ GeV/c and $\theta_{lab} = 4^\circ$ are 17, 38 and 16 times more than the one in the DIRAC experiment. The increased yields of the short-lived $\pi\pi(\pi K)$ atoms with minimum lifetime $\tau_{th} = 2.9 \cdot 10^{-15} s (\tau_{th} = 3.5 \cdot 10^{-15} s)$ allows to improve the precisions of their lifetime measurement and $\pi\pi(\pi K)$ scattering length combinations $|a_0 - a_2| (|a_{1/2} - a_{3/2}|)$.

In the DIRAC experiment the long-lived $\pi\pi$ atoms($\tau_{th} \geq 1.2 \cdot 10^{-11}$ s) were observed also. It was detected $n_A = 436 \pm 61$ $\pi^+\pi^-$ pairs(atomic pairs) originating in the breakup of long-lived $\pi\pi$ atoms in the Pt foil with probability more than 90%.

After the change of experiment scheme the number of produced long-lived $\pi^+\pi^-$, π^+K^- and $K^+\pi^-$ atoms per time unit at $P_p = 450$ GeV/c can be increased by 370, 1600 and 750 times accordingly. The background which gives the main contribution to the error in the n_A will be reduced two orders of magnitude. It allows to use the resonance method to measure the Lamb shift in $\pi\pi$ atom and the new $\pi\pi$ scattering length combination $2a_0 + a_2$. For the data analysis in the resonance method only Lorentz transformation and quantum mechanics will be used. The low energy QCD gives the precise predictions for values of $\pi\pi$ and πK scattering lengths and this precision will be improved in the future using Lattice calculations.

1 Introduction

The lifetime measurement of atoms consisting of K^+ and $\pi^-(A_{K\pi})$, K^- and $\pi^+(A_{\pi K})$ and π^+ and $\pi^-(A_{2\pi})$, allows to measure by model independent way the $\pi\pi$ and $K\pi$ scattering lengths [1, 2, 3, 4, 6]. The $A_{2\pi}$ were observed in p-Ta interactions at $P_P = 70$ GeV/c[5]. The experimental investigation of $A_{K\pi}$ and $A_{2\pi}$ atoms were done in the DIRAC experiment using the PS CERN proton beam with momentum $P_p = 24$ GeV/c[6, 7, 8, 9, 10]. The lifetime of short-lived $A_{2\pi}$ ($\tau_{th} = 2.9 \cdot 10^{-15} s$) connects with $\pi\pi$ s-wave scattering length combination $|a_0 - a_2|$, where 0 and 2 are the isospin values. In the DIRAC experiment the τ was measured [7, 8] with precision about 9% which gives for the combination of $|a_0 - a_2|$ accuracy of 4,3% (statistical error 3.1%) which is far away from the theoretical uncertainty of 1.5% [3]. Moreover at present time the lattice calculations significantly improved the accuracy of theoretical constants l_3 and l_4 which give the essential contribution into the accuracy. Therefore the precision of theoretical calculations of $\pi\pi$ scattering lengths can be improved.

The lifetime of short-lived $A_{\pi^+K^-}$ and $A_{K^+\pi^-}(\tau_{th} = 3.5 \cdot 10^{-15}s)$ connects with πK S-wave scattering length combination $|a_{1/2} - a_{3/2}|$, where 1/2 and 3/2 are the isospin values. The limited number of produced and detected short-lived $K\pi$ atoms allowed to evaluate the value of their lifetime and the value of $K\pi$ scattering length combination $|a_{1/2} - a_{3/2}|$ with precision 100% and 60% accordingly [9]. The precisions of theoretical prediction for values of $K\pi$ atom lifetime and for $K\pi$ scattering lengths are the 10% and 5% accordingly [11, 12, 13, 14].

The investigation of $A_{2\pi}$ allows to measure the Lamb shift in this atom [15, 16, 17] and to extract the another combination of $\pi\pi$ scattering lengths $2a_0 + a_2$ also. If the resonance method can be used then this combination will be obtained with precision of an order of magnitude higher than the accuracy of other methods[18, 19]. At the present time in the DIRAC experiment were observed 436±61 $\pi^+\pi^-$ pairs generating in the breakup of long-lived $A_{2\pi}$ in the Pt foil([10]).

The investigation of all the dimesoatoms was done using the two arm magnetic spectrometer with detectors which were placed before and after spectrometer magnet[20]. The particles generated in the target by primary proton beam moved in the solid angle of $1.2 \cdot 10^{-3}sr$ and crossed all the detectors before magnet. Positive and negative particles which crossed the detectors after the magnet had the momentum values in the interval of $1.2 \div 7GeV/c$. The flax of the secondary particles through the detectors restricts the primary proton beam intensity and atoms production per time unit. In the experiments on short-lived and long-lived dimesoatom investigation the primary proton beam intensity was 10^{11}protons/spill(the spill time is 0.45 s) and $3 \cdot 10^{11}$protons/spill accordingly. In the DIRAC experiments on the short-lived dimesoatoms investigation the atoms were generated in the Ni and Pt targets. Moving in the target the dimesoatoms interacted electromagnetically with target atoms and part of them was breaked up by producing $\pi^+\pi^-(K\pi)$ pairs with small relative momentum Q in the pair c.m.(atomic pair). The free $\pi^+\pi^-(K\pi)$ pairs were generating in the same target also. The small value of Q allows to identify the atomic pairs in the case of free pair background which was larger than atomic pair number more than an order of magnitude. This background gives the largest contribution to the error of atomic pair number.

In the DIRAC experiment on the long-lived $A_{2\pi}$ observation the atoms are produced in the Be target in the short-lived ns states. Moving in the target and interacting with Be atom electromagnetically some part of the $A_{2\pi}$ leaves the target in the exited long-lived states with different quantum numbers. These atoms in the momentum interval of $2.5 \div 10.5$ GeV/c have the decay length in the l.s. from a few centimeters up to 3.4 meters[15]. At the distance of 96 mm downstream of the target there was installed the 2.1 μ Pt foil in which more than 90% of long-lived atoms are breaked up by generating atomic $\pi^+\pi^-$ pairs. The week magnetic field between Be target and Pt foil was applied to enlarge the vertical component Q_Y of the relative momentum Q in the c.m of the $\pi^+\pi^-$ pairs generating in Be target. The increased Q_Y allows to suppress the background of $\pi\pi$ pairs produced in Be target. But this magnetic field practically did not reduce the flax of the charged particles into the setup aperture.

It is obvious that for the investigation of $K\pi$ atoms, $\pi\pi$ atom Lamb shift measurement and lifetime accuracy improvement the detected number of atoms must be enlarged more than an order of magnitude. The significantly increased dimesoatom yields at growth of P_p from 24 GeV/c up to 450 GeV/c(on the SPS CERN) was established in [21, 22, 23]. In [23] the yields and spectra of $A_{2\pi}$, $A_{\pi^+K^-}$ and $A_{\pi^-K^+}$ generated in p-Ni interactions

at $P_p = 24$ and 450 GeV/c were calculated a bit precisely than in [21, 22]. Because the yields of $A_{\pi^+K^-}$, $A_{\pi^-K^+}$ and $A_{2\pi}$ at $P_p = 24$ GeV/c and $\theta_{lab} = 5.7^\circ$ are measured now, the ratio of these atom yields at $P_p = 450$ GeV/c, $\theta_{lab} = 0 \div 5.7^\circ$ and at $P_p = 24$ GeV/c were calculated. It allows to determine the optimal value of θ_{lab} at 450 GeV/c and expected statistics of $A_{2\pi}$ and $A_{\pi K}$.

In [23] to obtain the yields of $K^{\pm}$- and $\pi^{\pm}$-mesons the computer simulation programs FRITIOF 6.0 and JETSET 7.3 [24] (CERN Program Library) based on the Lund string fragmentation model were used. FRITIOF is a generator for hadron-hadron, hadron-nucleus and nucleus-nucleus collisions which makes use of JETSET for fragmentation.

In the present work the calculations were performed using FTF generator [25] - the developed version of FTITIOF generator for GEANT4[26]. Experimental data on K^+, K^-, π^+ and π^- production inclusive cross sections at proton momentum of 31 GeV/c(p-C)[28] were compared with the generator predictions and were used to evaluate the FTF precision at P_p =31 GeV/c. This precision in the momentum and angular intervals coinciding with the DIRAC experiment intervals were used as a accuracy of FTF description of the same cross sections in p-Ni interactions at 24 GeV/c. The FTF accuracy at 450 GeV/c was checked only in the laboratory angle interval $0 \div 1.7^\circ$ where the experimental data are existing[29]. The absolute and relative dimesoatom yields at 450 GeV/c as a function of θ_{lab} and atom momentum were calculated. It allows to obtain the number of detected short-lived and long-lived dimesoatoms and expected statistical errors. Also the experimental data from p-C and p-Cu interactions at proton momentum of 100 GeV/c[30] were compared with the generator predictions to make the conclusion about FTF possibility to describe inclusive cross sections for both nuclei.

2 Basic relations

The probability of atom production is proportional to the double inclusive cross section for generation of the two constituent particles of this atom with small relative momenta. Calculating the atom production cross section, one should exclude the contribution to the double cross section from those constituents that arise from the decays of long-lived particles and can not form the atom. When one or both particles in the pair come from these decays the typical range between them is much larger than the Bohr radius of the atom 249 fm for $A_{\pi K}$) and (387 fm for $A_{2\pi}$ then the probability of atom production is negligible. The main long-lived sources of pions are η and η'. For the case of pions and kaons the short-lived sources constitute the main contribution.

The laboratory differential inclusive cross section for the atom production can be written in the form [15]

$$\frac{d\sigma_n^A}{d\vec{p}_A} = (2\pi)^3 \frac{E_A}{M_A} |\Psi_n(0)|^2 \left. \frac{d^2\sigma_s}{d\vec{p}_1\, d\vec{p}_2} \right|_{\vec{p}_1 = \frac{m_1}{m_2}\vec{p}_2 = \frac{m_1}{M_A}\vec{p}_A}, \qquad (1)$$

where M_A is the atom mass, $\vec{p}_A$ and E_A are the momentum and energy of the atom in the lab system, respectively, $|\Psi_n(0)|^2 = p_B^3/\pi n^3$ is the atomic wave function (without regard for the strong interactions between the particles forming the atom, i.e. the pure Coulomb wave function) squared at the origin with the principal quantum number n and the orbital momentum $l = 0$, p_B is the Bohr momentum of the particles in the atom,

$d^2\sigma_s^0/d\vec{p}_1 d\vec{p}_2$ is the double inclusive production cross section for the pairs from short-lived sources (hadronization processes, ρ, ω, Δ, K^*, Σ^*, etc.) without regard for the $\pi^+\pi^-$ ($K^+\pi^-$, $K^-\pi^+$) Coulomb interaction in the final state, $\vec{p}_1$ and $\vec{p}_2$ are the momenta of the particles forming the atom in the lab system. The momenta obey the relation $\vec{p}_1 = \frac{m_1}{m_2}\vec{p}_2 = \frac{m_1}{M_A}\vec{p}_A$ (m_1 and m_2 are the masses of the particles). The atoms are produced with the orbital momentum $l = 0$, because $|\Psi_{n,l}(0)|^2 = 0$ when $l \neq 0$. The atoms are distributed over n as n^{-3}: $W_1 = 83\%$, $W_2 = 10.4\%$, $W_3 = 3.1\%$, $W_{n\geq 4} = 3.5\%$. Note that $\Sigma_{n=1}^{\infty}|\Psi_n(0)|^2 = 1.202|\Psi_1(0)|^2$.

After substituting the expression for $|\Psi_n(0)|^2$ and summing over n, one can obtain an expression for the inclusive yield of atoms in all S-states through the inclusive yields of positive and negative hadron pairs

$$\frac{d\sigma^A}{d\vec{p}_A} = 1.202 \cdot 8\,\pi^2\,(\mu\alpha)^3\,\frac{E_A}{M_A}\,\left.\frac{d^2\sigma_s}{d\vec{p}_1\,d\vec{p}_2}\right|_{\vec{p}_1=\frac{m_1}{m_2}\vec{p}_2=\frac{m_1}{M_A}\vec{p}_A}, \tag{2}$$

where μ is the reduced mass of the atom ($\mu = \frac{m_1 m_2}{m_1+m_2}$), α is the fine structure constant.

Instead of differential cross section it is convenient to introduce the probability of particle production per one inelastic interaction (yield):

$$\frac{dN}{d\vec{p}} = \frac{d\sigma}{d\vec{p}}\,\frac{1}{\sigma_{in}}, \qquad \frac{d^2N}{d\vec{p_1}d\vec{p_2}} = \frac{d^2\sigma}{d\vec{p_1}d\vec{p_2}}\,\frac{1}{\sigma_{in}}, \tag{3}$$

where σ_{in} is the inelastic cross section of hadron production.

Then

$$\frac{dN_A}{d\vec{p}_A} = 1.202 \cdot 8\,\pi^2\,(\mu\alpha)^3\,\frac{E_A}{M_A}\,\left.\frac{d^2N_s}{d\vec{p}_1\,d\vec{p}_2}\right|_{\vec{p}_1=\frac{m_1}{m_2}\vec{p}_2=\frac{m_1}{M_A}\vec{p}_A}, \tag{4}$$

The double yield(without regard for the Coulomb interaction) can be presented as [31]:

$$\frac{d^2N_s}{d\vec{p}_1 d\vec{p}_2} = \frac{dN_1}{d\vec{p}_1}\,\frac{dN_2}{d\vec{p}_2}\,R(\vec{p_1},\vec{p_2},S), \tag{5}$$

where $dN_1/d\vec{p}_1$ and $dN_2/d\vec{p}_2$ are the single particle yields, R is a correlation function due to strong interaction only and S is the square of full c.m.s. energy of beam proton and target hadron.

The yield and momentum distribution of $A_{2\pi}$ were measured[8] at $P_p = 24$ GeV/c and $\theta_{lab} = 5.7^\circ$, the yields of π^+K^- and $K^+\pi^-$ atoms at the same proton momentum and angle were obtained in [9]. Hence it is useful to present not only the absolute yields of atoms at different conditions but their yields relative to the known values.

3 Experimental values of pion and kaon inclusive cross sections and their description by FTF.

It is important to know how well the inclusive cross sections obtained by FTF coincide with corresponding experimental data at proton momentum $P_P = 24$ and 450 GeV/c. In the DIRAC experiment of $A_{2\pi}$ measurement the main interval of pion momentum in $\pi^+\pi^-$ atomic pairs is $1 \div 3$ GeV/c and for kaons from $A_{\pi K}$ breakup is $4 \div 7$ GeV/c. We

are going to use Ni target but there is no data for pion and kaon inclusive cross sections for such material. The data [32] reveals the weak dependence of soft pion and kaon yields on the nucleon atomic number A from Be up to Cu. Also there is the weak dependence of these yields on A in p-nucleus (C, Al, Cu) interactions at $P_p = 100$ GeV/c for the secondary particle momentum of 30 GeV/c[30]. Therefore the soft particle experimental yields in carbon and Be can be used to check the FTF precision and to use this accuracy for the generator predictions for p-Ni interactions. The values of soft dimesoatom yields calculated and measured for p-Ni interactions are a good estimation of the same yields in any p-nucleus interaction.

3.1 Comparison of experimental inclusive cross sections in p-C interactions at $P_p = 31$ GeV/c with FTF predictions.

The inclusive cross sections of π^+, π^-, K^+ and K^- in p-C interactions at $P_p = 31$ GeV/c. were measured [28] with high precision and compared with VENUS, EPOS and GiBUU predictions.

The Fig.1-4 present the experimental and calculated inclusive yield values of π^+, π^-, K^+ and K^- as a function of particle momentum in l.s.. The intervals of π^+ and π^- polar angle θ_{lab} in l.s. from 60÷100 $mrad$ and 100÷140 $mrad$ fully cover the θ_{lab} interval of the DIRAC setup (82÷116 $mrad$). From Fig.1 and 2 we can see that the FTF describes the inclusive cross sections in the momentum interval 1÷3 GeV/c better than 10%. With the same precision the FTF describes π^+ and π^- inclusive cross sections [27] in the interval $0 \leq \theta_{lab} \leq 420$ $mrad$ investigated in the experiment[28].

For K^+ inclusive yields in wide θ_{lab} interval 20÷140 $mrad$ (Fig.3) the calculated values are 30% higher than experimental ones. But in the θ_{lab} interval 140÷240 $mrad$ (Fig.3) where P_t are relatively large the agreement is good. Therefore it is possible that the FTF describes the experimental data in the interval 82÷116 $mrad$ with relatively high P_t better than in the hole interval 20÷140 $mrad$. In this case the 30% precision is the upper limit of the inclusive cross section uncertainty.

For K^- in the interval 60÷140 $mrad$ the calculated values are ≈15 % higher than the experimental data (Fig.4) at P_K =4 GeV/c and ≈100 % at $P_K = 7$ GeV/c.

3.2 Comparison of experimental inclusive cross sections in p-nucleus interactions at $P_p = 450$ GeV/c and $P_p = 100$ GeV/c with FTF predictions.

The invariant inclusive cross sections of π^+, π^-, K^+ and K^- in p-Be interactions at $P_p =$ 450 GeV/c were measured [29] and compared with FTF predictions in [27]. It follows that the generator describes well the inclusive cross sections of π^+ and π^- up to momentum of 70 GeV/c(Fig.5). Therefore generator can be used for description of $A_{2\pi}$ yields up to momentum of 140 GeV/c.

The inclusive cross sections of K mesons are described with precision about 20% up to momentum of 20 GeV/c and 40 GeV/c for K^+ and K^- accordingly(Fig.5). It allows to calculate the yields of $A_{K\pi}$ and $A_{\pi K}$ up to momentum of 26 GeV/c and 51 GeV/c accordingly.

The data on dependence of experimental inclusive yields of π and K mesons with momentum $P = 15$ GeV/c and $P = 40$ GeV/c on P_t is described[27] by FTF well(Fig.6).

The data on inclusive production of π^+, π^-, K^+ and K^- in p-C and p-Cu interactions at $P_p = 100$ GeV/c were measured [30] and compared with FTF predictions in [27]. The conclusion is that the FTF does not describe experimental data at large values of x for p-C interactions. The discrepancy between FTF predictions and p-Cu experimental data is less than in p-C interactions. It can be considered as the indication that the yield of dimesoatoms at $P_p = 450$ GeV/c from Ni target can be described by FTF not worth than from Be target.

4 Results of calculations

The selection of particles from long-lived and short-lived sources was performed. Further, using yields from the short-lived sources only we obtained the double inclusive yields of $\pi^+\pi^-$, $K^+\pi^-$ and $K^-\pi^+$ pairs and the dependence of corresponding atom yields over their angle and momentum in l.s..

It is important to know the ratio between number of dimesoatoms and the full flax of charged particles in the same solid angle which is seven orders of magnitude more than the number of atoms. This flax of charged particles restricts the intensity of the primary proton beam and the number of generating atoms per time unit. Therefore for each angle and proton momentum the yield of charged particles was calculated also.

4.1 Calculations of inclusive yields of charged particles, $\pi\pi$ and πK atoms.

In this part the yield calculations was done in the solid angle of $10^{-3}sr$ without taking into account the setup acceptance and particle decays.

On the Fig.7 the total yields of charged particles ($\pi^{\pm}$, $K^{\pm}$, p and $\bar{p}$) per one p-Ni interaction at the proton momentum of 450 GeV/c and emission angles $\theta_{lab} = 0^{\circ}$, 2°, 4°(bottom) and at the proton momentum of 24 GeV/c and emission angle $\theta_{lab} = 5.7^{\circ}$(top) as a function of their momentum are shown.

On the Fig.8 there are the yields of all the atoms into solid angle of 10^{-3} sr. On Fig.9 the same yields of $A_{2\pi}$, $A_{\pi^+K^-}$ and $A_{K^+\pi^-}$ as their momentum function are presented in the intervals 2.5÷10.5 GeV/c($A_{2\pi}$) and 5÷14 GeV/c ($A_{\pi K}$). The chosen intervals are the working intervals of the DIRAC setup in which the identification of charged particle is really simple. In the Tab.1 these yields integrated over P_A are shown, where W_{ch} and W_A are the total yields of charged particles ($\pi^{\pm}$, $K^{\pm}$, p, $\bar{p}$) and $\pi^+\pi^-$, π^+K^-, $K^+\pi^-$ atoms accordingly into the aperture of 10^{-3} sr per one p-Ni interaction. The relative yields of charged particles and atoms are W_{ch}^N=$W_{ch}/W_{ch}(5.7^{\circ}, 24\ GeV/c)$ and W_A^N=$W_A/W_A(5.7^{\circ}, 24\ GeV/c)$). The yield values of $A_{2\pi}$ and $A_{\pi K}$ are practically the same as in [23] where the FRITIOF 6 was used for calculations.

At $\theta_{lab} = 4^{\circ}$ and P_p=450 GeV/c the yields of $\pi^+\pi^-$, π^+K^- and $K^+\pi^-$ atoms are 17, 37 and 16 times more respectively than at $\theta_{lab} = 5.7^{\circ}$ and P_p=24 GeV/c. These yields increase two times at $\theta_{lab} = 2^{\circ}$.

Table 1: The total yield of charged particles ($\pi^{\pm}$, $K^{\pm}$, p and $\bar{p}$) W_{ch}, $\pi^+\pi^-$, π^+K^- and $K^+\pi^-$ atoms W_A into the aperture of 10^{-3} sr per one p-Ni interaction at the proton momenta P_p = 24 and 450 GeV/c versus emission angle θ_{lab} and in the intervals 2.5÷10.5 GeV/c($A_{2\pi}$) and 5÷14 GeV/c ($A_{\pi K}$) without taking into account the decays of pions and kaons in the setup. The relative yields of charged particles and atoms are W_{ch}^N=$W_{ch}/W_{ch}(5.7^\circ, 24\ GeV/c)$ and W_A^N=$W_A/W_A(5.7^\circ, 24\ GeV/c)$.

θ_{lab}	5.7°	4°	2°	0°
P_p	24 GeV/c	450 GeV/c	450 GeV/c	450 GeV/c
The yield of charged particles				
W_{ch}	0.022	0.14	0.50	2.9
W_{ch}^N	1	6.4	22.7	132
The yield of $\pi^+\pi^-$ atoms				
W_A	$1.94{\cdot}10^{-9}$	$3.4{\cdot}10^{-8}$	$6.9{\cdot}10^{-8}$	$8.9{\cdot}10^{-8}$
W_A^N	1	17.3	35.4	45.9
The yield of π^+K^- atoms				
W_A	$2.17{\cdot}10^{-10}$	$8.1{\cdot}10^{-9}$	$1.63{\cdot}10^{-8}$	$2.3{\cdot}10^{-8}$
W_A^N	1	37.5	75.	106.
The yield of $K^+\pi^-$ atoms				
W_A	$5.2{\cdot}10^{-10}$	$8.5{\cdot}10^{-9}$	$1.9{\cdot}10^{-8}$	$3.0{\cdot}10^{-8}$
W_A^N	1	16.4	37.6	57.4

4.2 Calculations of inclusive yields of $\pi\pi$ and πK atoms detected by setup

The experimental investigation of $A_{2\pi}$, $A_{\pi^+K^-}$ and $A_{K^+\pi^-}$ was done in the DIRAC experiment. The acceptance of the DIRAC setup without taking into account the particle decays is presented on Fig.11. For the case P_p = 450 GeV/c we used the same acceptance to obtain the yield values which allows to calculate the expected number of $A_{2\pi}$, $A_{\pi^+K^-}$ and $A_{K^+\pi^-}$ using the DIRAC experiment data.

On Fig.11 the yields of $A_{\pi^+K^-}$, $A_{K^+\pi^-}$ and $A_{2\pi}$ per one p-Ni interaction into solid angle of 10^{-3} sr as a function of these atom momentum and with taking into account the setup acceptance are presented. These yields are for proton momentum of 450 GeV/c, emission angles θ_{lab} = 0°, 2°, 4° and for proton momentum of 24 GeV/c and emission angle θ_{lab} = 5.7° .

In the Tab.2 these yields integrated over P_A are shown. There are shown the absolute values of atomic yields, their relative values when their yield at 24 GeV/c and 5.7° is set to 1 and their values relative to the flux of charged particles in the DIRAC channel. The last values are important as in the channel there are the forward detectors which should operate at this flux of charged particles. Also this ratio is less sensitive to the accuracy of the meson production inclusive cross sections than the atomic absolute yield.

At θ_{lab} = 4° and P_p=450 GeV/c where charged particle momenta are small and their identification is relatively simple the yields of $\pi^+\pi^-$, π^+K^- and $K^+\pi^-$ atoms are 15, 67 and 31 times more respectively , than at θ_{lab} = 5.7° and P_p=24 GeV/c. It means that

Table 2: The yield of $\pi^+\pi^-$, π^+K^- and $K^+\pi^-$ atoms W_A into the aperture of 10^{-3} sr taking into account the setup acceptance and pion and kaon decays per one p-Ni interaction at the proton momenta P_p = 24 and 450 GeV/c versus emission angle θ_{lab}. W_A^N=$W_A/W_A(5.7^\circ, 24\ GeV/c)$ and $(W_A/W_ch)^N$=$(W_A/W_ch)/((W_A/W_ch)(5.7^\circ, 24\ GeV/c))$.

θ_{lab}	5.7°	4°	2°	0°
E_p	24 GeV/c	450 GeV/c	450 GeV/c	450 GeV
The yield of $\pi^+\pi^-$ atoms				
W_A	$1.25{\cdot}10^{-9}$	$1.9{\cdot}10^{-8}$	$3.5{\cdot}10^{-8}$	$4.5{\cdot}10^{-8}$
W_A^N	1	15	28	36
W_A/W_{ch}	$5.70{\cdot}10^{-8}$	$1.4{\cdot}10^{-7}$	$7.{\cdot}10^{-8}$	$1.6{\cdot}10^{-8}$
$(W_A/W_{ch})^N$	1	2.4	1.2	0.27
The yield of π^+K^- atoms				
W_A	$1.3{\cdot}10^{-11}$	$8.8{\cdot}10^{-10}$	$1.7{\cdot}10^{-9}$	$2.0{\cdot}10^{-9}$
W_A^N	1	67	131	154
W_A/W_{ch}	$5.9{\cdot}10^{-10}$	$6.3{\cdot}10^{-9}$	$3.4{\cdot}10^{-9}$	$6.9{\cdot}10^{-10}$
$(W_A/W_{ch})^N$	1	10.6	5.8	1.2
The yield of $K^+\pi^-$ atoms				
W_A	$3.1{\cdot}10^{-11}$	$9.7{\cdot}10^{-10}$	$2.1{\cdot}10^{-9}$	$2.7{\cdot}10^{-9}$
W_A^N	1	31	68	87
W_A/W_{ch}	$1.4{\cdot}10^{-9}$	$6.9{\cdot}10^{-9}$	$4.2{\cdot}10^{-9}$	$9.3{\cdot}10^{-10}$
$(W_A/W_{ch})^N$	1.	4.9	3.0	0.66

it is possible to decrease the proton beam intensity to obtain the reduction of trigger events with accidental coincidences. The additional increasing of the atom production is connected with beam time during supercycle on PS and SPS. At best condition the DIRAC experiment had on PS the 4 spills with duration 0.45 s (full time 1.8 s). On SPS during the same supercycle the beam time is 4.6*2 = 9.6 s which gives the increasing for the atom production per time unit more than 5. With this additional increasing the number of produced atoms at the same intensity of secondary particles is more than an order of magnitude greater than at P_P = 24 GeV/c.

We can notice that at P_p=450 GeV/c the soft proton background is more than an order of magnitude less than at 24 GeV/c [32, 29] decreasing an order of magnitude the background of $p\pi^-$ pairs relative to the $K^+\pi^-$ pairs.

4.3 Calculations of correlation function $R(\vec{p_1}, \vec{p_2}, S)$ at proton momentum of 24 and 450 GeV/c for π^+K^-, $K^+\pi^-$ and $\pi^+\pi^-$ pairs with small relative momentum.

The differential inclusive yield of atom production in (4) is expressed through double differential yield of two constituent particles. This yield we obtained using FTF generator. We can use the FTF to determine the correlation function (5) which allows to evaluate the uncertainty in W_A^N minimum value. This factor for the momentum interval of the DIRAC

setup is presented on Fig.12. It shows that the factor R for $\pi^+\pi^-$ pairs at P_p=24 GeV/c decreases from 1.25 (P_{pair} = 3 GeV/C) up to 0.5 (P_{pair} = 9 GeV/c). For $K\pi$ pairs R decreased from 1 (3 GeV/c) up to 0.5 (10 GeV/c). This decreasing is partially due to conservation low constrains. At P_p = 450 GeV/c the value of R practically does not depend on pair momentum and polar angle.

On Fig.12 we see that for all kinds of pairs the correlation function R at $P_p = 24$ GeV/c is less for all particle momentum than the one at P_p = 450 GeV/c. The calculating of relative atom yields W_A^N with putting the correlation function R to 1 gives us the minimum value of W_A^N. In this case the error of W_A^N depends only on the uncertainties of inclusive cross section description by FTF. These uncertainties can be evaluated from experimental data analysis.

5 On the accuracy of FTF simulation results.

In the equation (5) the double yield is presented via the product of two single particle yields and a correlation factor R. It was shown(chapter 4.3) that if $R = 1$ then the minimum relative yield value $W_A(R = 1)^N$ is obtained. In this case the error in $W_A(R = 1)^N$ depends only on the uncertainty in the single particle yield description by FTF which we can obtain from experimental distributions(Fig.1-6).

In the case of $A_{2\pi}$ for $P_p = 24$ GeV/c we compared for MC and experimental data the product of π^+ and π^- distributions(Fig.1) in the pion momentum interval of 1$\div$3 GeV/c and for polar angle of 60$\div$100 $mrad$. The ratio of products $K_{24\pi^+\pi^-} = PROD^{exp}_{24\pi^+\pi^-}/PROD^{MC}_{24\pi^+\pi^-}$ = 1.16$\pm$0.06.

In the case of $A_{K^+\pi^-}$ for P_p = 24 GeV/c we compared for MC and experimental data the product of K^+(Fig.3, 20$\div$140 $mrad$) and π^- distributions(Fig.1, 60$\div$100 $mrad$) in the kaon momentum interval of 4$\div$7 GeV/c. The ratio of products $K_{24K^+\pi^-} = PROD^{exp}_{24K^+\pi^-}/PROD^{MC}_{24K^+\pi^-}$ = 0.78$\pm$0.06.

In the case of $A_{K^-\pi^+}$ for P_p = 24 GeV/c we compared for MC and experimental data the product of K^-(Fig.4, 100$\div$140 $mrad$) and π^+ distributions(Fig.1, 60$\div$100 $mrad$) in the kaon momentum interval of 4$\div$7 GeV/c. The ratio of products $K_{24K^-\pi^+} = PROD^{exp}_{24K^-\pi^+}/PROD^{MC}_{24K^-\pi^+}$ = 0.90$\pm$0.07.

For P_p = 450 GeV/c we used the point in experimental invariant inclusive cross sections of π^+, π^-, K^+ and K^- at P_{π^+,π^-,K^+,K^-} = 7 GeV/c.

The same ratios for P_p = 450 GeV/c($K_{450\pi^+\pi^-}$,$K_{450K^+\pi^-}$ and $K_{450K^-\pi^+}$) are equal 0.87$\pm$0.13, 0.75$\pm$0.12 and 0.82$\pm$0.17 correspondingly.

We used these correction factors to estimate the minimal gain of atom production at P_p = 450 GeV/c with comparison with P_p = 24 GeV/c (Tab.3,4).

The $W_A(R = 1)$ and $W_A(R = 1)^N$ values are presented in Tab.3. At P_P = 450 GeV/c the minimum ratios of $A_{2\pi}$, $A_{\pi^+K^-}$ and $A_{\pi^-K^+}$ equal to 9.7 ± 1.5, 45 ± 8 and 18.6 ± 4.1 correspondingly confirming that even minimum yields of $A_{\pi^+K^-}$ and $A_{\pi^-K^+}$ at P_P = 450 GeV/c are large more an order of magnitude that the yields at P_P = 24 GeV/c.

6 The prospects of long-lived dimesoatom investigation at P_p = 450 GeV/c and the long-lived dimesoatom beam creation.

As mentioned in the introduction the secondary particle flax intensity restricts the primary proton beam intensity at experiment on the long-lived $A_{2\pi}$ observation on the level of $3 \cdot 10^{11}$ protons/spill(time of spill = 0.45 s) and the number of atoms produced in the time unit. The atoms production in the time unit can be increased significantly if after Be target to install a collimator and to apply after it the vertical magnetic field with BL deflecting from the setup aperture the soft particles with momentum less than 10 GeV/c. In this case the total flax of the secondary charged particles into the setup aperture at angle of 4° is decreased 5 times(Fig.7) and hence the intensity of primary proton beam and the number of produced atoms can be enlarged 5 times. In this scheme the number of generated long-lived $A_{2\pi}$, $A_{\pi^+K^-}$ and $A_{\pi^-K^+}$ at P_p = 450 GeV/c and $\theta_{lab} = 4°$ per unit time will be 370, 1600, and 750 times more than at P_p = 24 GeV/c and $\theta_{lab} = 5.7°$.

In the DIRAC experiment using 2/3 of statistics n_{AL} = 436±57stat±23syst atomic pairs from the long-lived atom breakup in the Pt foil were detected. The main contribution into the statistical error gives the background of $\pi^+\pi^-$ pairs generating in Be target. This background is 40 times more than n_{AL}. After magnetic field applying the charged particles with momentum less than 10 GeV/c will not be detected by detectors of setup which are after spectrometer magnet and the background will be decreased very significantly. In the experiments on the $\pi\mu$ atom observation and investigation at the conditions close much to the scheme with magnetic field the background was at the level of a few percent relative to $\pi\mu$ pairs from atom breakup in the thin foil[34].

Therefore with applied magnetic field the error of n_{AL} will be significantly less than in the DIRAC experiment and it is not only as result of atomic pair statistic increasing by more than two orders of magnitude but also as result of the background suppression by more than two orders of magnitude. The main source of the systematic error in n_{AL} is the thickness of Pt foil uncertainty which can be decreased significantly.

In the experiment when some part of charged particles is deflected from the setup aperture by additional magnetic field the number of detected $\pi+\pi-$ atomic pairs per time unit will be increased less than the number of produced long-lived atoms. In this scheme the distance between Be target and Pt foil is larger than in the DIRAC experiment(96 mm) and part of the long-lived atoms decays before the foil. The decay probability for the part of the atoms with orbital momentum projection in the magnetic field direction $m = 0$ is increased also by magnetic field. Nevertheless the number of detected atomic pairs per time unit will be larger two orders of magnitude than in the DIRAC experiment. The large statistics of atomic pairs and background low level open the possibility to use the resonance method[17] for the $A_{2\pi}$ Lamb shift measurement.

In this method the long-lived atoms are crossing an electric or magnetic field which is a periodic function of the coordinate along the beam axis with frequency ω_L. In the atom c.m. this field is transformed into an electric field which is oscillating in time with the frequency $\tilde{\omega} = \omega_L\gamma$, where γ is the atom Lorentz factor. For the set of γ the value of $\tilde{\omega}$ coincides with the atom own frequencies $\Omega_n = (E_{np} - E_{ns})/\hbar$, where E_{ns} and E_{np} are the atomic level energies and $\hbar$ is Planck constant. In this case the atoms with the values

of Lorentz factors from equation

$$\gamma_n \omega_L = \Omega_n \tag{6}$$

oscillate between $np - ns$ states. The short-lived ns-state atoms decay completely and the number of dimesoatoms after resonator with Lorentz factors around γ_n is decreased.

After resonator a thin Pt foil will be installed in which more than 90% of long-lived atoms are breaked up. In the momentum spectrum of atomic pairs the set of minima will present also . Measuring the positions of γ_n minima and knowing the resonator frequency ω_L we can evaluate from equation (6) the energy splitting between $np-ns$ states. The part of the energy splitting connecting with the vacuum polarization and other electromagnetic effects are about 20% of the total energy splitting. After this part subtraction the strong part of the energy splitting depending on the $\pi\pi$ scattering length combination $2a_0 + a_2$ will be obtained . The difference of this method from other methods of $\pi\pi$ scattering length evaluation is that the measurement of the total energy splitting uses only Lorentz transformation and quantum mechanics in the experimental data analysis.

Large yield of $A_{\pi^+K^-}$ and $A_{\pi^-K^+}$ allows to observe these atoms simultaneously with $A_{2\pi}$ Lamb shift measurement using symmetrical setup geometry which is optimal only for $\pi^+\pi^-$ atomic pair detection. The $A_{\pi^+K^-}$ and $A_{\pi^-K^+}$ energy splitting measurement can be done in the asymmetric geometry of the setup taking into account that in πK atomic pairs the K meson momentum is 3.6 times more than the pion momentum.

In the DIRAC experiments on the dimesoatom investigation the thin targets were used with the nuclear efficiency $2.5 \cdot 10^{-4}$ for the long-lived atoms and $6.5 \cdot 10^{-4}$ for the short-lived atoms. Therefore these experiments disturb the proton beam insignificantly and can be performed simultaneously with the other experiments.

Table 3: The yield $W_A(R=1)$ of $\pi^+\pi^-$, π^+K^- and $K^+\pi^-$ atoms with $R=1$ into the aperture of 10^{-3} sr taking into account the setup acceptance and pion and kaon decays per one p-Ni interaction at the proton momenta $P_p = 24$ and 450 GeV/c versus emission angle θ_{lab}. The ratio $(W_A(R=1))^N = W_A(R=1,\ 450\ GeV/c)/W_A(R=1,\ 5.7°, 24\ GeV/c)$ gives the minimum value of ratio of atom yields at $P_p = 450$ GeV/c and $P_p = 24$ GeV/c.

θ_{lab}	5.7°	4°	2°	0°
E_p	24 GeV/c	450 GeV/c	450 GeV/c	450 GeV
The yield of $\pi^+\pi^-$ atoms				
$W_A(R=1)$	$(1.73 \pm 0.09) \cdot 10^{-9}$	$(1.7 \pm 0.2) \cdot 10^{-8}$	$(3.0 \pm 0.5) \cdot 10^{-8}$	$(3.9 \pm 0.6) \cdot 10^{-8}$
$(W_A(R=1))^N$	1	9.7 ± 1.5	17.5 ± 2.8	22.7 ± 3.6
The yield of π^+K^- atoms				
$W_A(R=1)$	$(1.46 \pm 0.09) \cdot 10^{-11}$	$(6.6 \pm 1.1) \cdot 10^{-10}$	$(1.31 \pm 0.21) \cdot 10^{-9}$	$(1.52 \pm 0.24) \cdot 10^{-9}$
$(W_A(R=1))^N$	1	45 ± 8	87 ± 15	104 ± 18
The yield of $K^+\pi^-$ atoms				
$W_A(R=1)$	$(4.2 \pm 0.3) \cdot 10^{-11}$	$(7.9 \pm 1.6) \cdot 10^{-10}$	$(1.8 \pm 0.4) \cdot 10^{-9}$	$(2.2 \pm 0.5) \cdot 10^{-9}$
$(W_A(R=1))^N$	1	18.6 ± 4.1	41 ± 9	52 ± 11

Table 4: The relative yields $W_A(R=1)/W_{ch}$ of $\pi^+\pi^-$, π^+K^- and $K^+\pi^-$ atoms into the aperture of 10^{-3} sr taking into account the setup acceptance and pion and kaon decays per one p-Ni interaction at the proton momenta $P_p = 24$ and 450 GeV/c versus emission angle θ_{lab}. $(W_A(R=1)/W_{ch})^N$=$(W_A(R=1)/W_{ch})/((W_A(R=1)/W_{ch})(5.7°, 24\ GeV/c))$.

θ_{lab}	5.7°	4°	2°	0°
E_p	24 GeV/c	450 GeV/c	450 GeV/c	450 GeV
The yield of $\pi^+\pi^-$ atoms				
$W_A(R=1)/W_{ch}$	$7.8 \pm 0.4) \cdot 10^{-8}$	$(1.21 \pm 0.14) \cdot 10^{-7}$	$(6.0 \pm 1.0) \cdot 10^{-8}$	$(1.34 \pm 0.21) \cdot 10^{-8}$
$(W_A(R=1)/W_{ch})^N$	1	1.55 ± 0.20	$0.77 \pm /13$	$.17 \pm 0.03$
The yield of π^+K^- atoms				
$W_A(R=1)/W_{ch}$	$(6.6 \pm 0.4) \cdot 10^{-10}$	$(4.7 \pm 0.8) \cdot 10^{-9}$	$(2.6 \pm 0.4) \cdot 10^{-9}$	$(5.2 \pm 0.8) \cdot 10^{-10}$
$(W_A(R=1)/W_{ch})^N$	1	$7. \pm 1.$	3.9 ± 0.7	0.79 ± 0.13
The yield of $K^+\pi^-$ atoms				
$W_A(R=1)/W_{ch}$	$(1.91 \pm 0.14) \cdot 10^{-9}$	$(5.6 \pm 1.1) \cdot 10^{-9}$	$(3.6 \pm 0.8) \cdot 10^{-9}$	$(7.6 \pm 1.7) \cdot 10^{-10}$
$(W_A(R=1)/W_{ch})^N$	1	2.9 ± 0.6	1.9 ± 0.4	0.40 ± 0.09

7 Conclusion

The performed analysis shows that the atom production in the p-nucleus interaction increases more than an order of magnitude if the momentum of the proton P_p changes from 24 GeV/c up to 450 GeV/c. The yield of $A_{2\pi}(A_{\pi^+K^-}, A_{\pi^-K^+})$ in the momentum interval of the DIRAC experiment 2.5÷10.5 GeV/c(5÷14 GeV/c) at P_p = 450 GeV/c and $\theta_{lab} = 4^\circ$ increases 17(38, 16) times relative to all these atom productions at P_p = 24 GeV/c and $\theta_{lab} = 5.7^\circ$(Tab.1). The yield values increases twice if $\theta_{lab} = 2^\circ$. All these values were calculated by integration of dedicated atomic momentum spectrum in the intervals mentioned above. If with this integration take into account the DIRAC setup acceptance (Tab.2) then the relative yields of $A_{2\pi}$, $A_{\pi^+K^-}$ and $A_{\pi^-K^+}$ at $\theta_{lab} = 4^\circ(2^\circ)$ are 15(28), 67(131) and 31(68) correspondingly. The minimum values of these yields were evaluated by model independent way and the following numbers(Tab.3) at $\theta_{lab} = 4^\circ(2^\circ)$ were obtained: 9.7±1.5(17.5±2.8), 45±8(87±15) and 18.6±4.1(41±9) confirming that even minimum yields increase more than an order of magnitude.

In the experiments on lifetime measurement of short-lived $A_{2\pi}$, $A_{\pi^+K^-}$ and $A_{\pi^-K^+}$ the secondary particle flax intensity in the DIRAC experiment restricted the primary proton beam intensity and the number of detected atoms in the time unit. For the same total flax intensity of charged particles like in the DIRAC experiment the yields of $A_{2\pi}$, $A_{\pi^+K^-}$ and $A_{\pi^-K^+}$ at P_p = 450 GeV/c and $\theta_{lab} = 4^\circ$ increases 2.7, 5.8 and 2.5 times accordingly. As mentioned in the chapter 4.2 the beam time per supersycle on SPS is 5 times more than on PS. Therefore the number of $A_{2\pi}$, $A_{\pi^+K^-}$ and $A_{\pi^-K^+}$ per time unit increases 14, 29 and 12 times accordingly.

In the DIRAC experiment, in p-Be interactions, using of 2/3 of existing statistics, the 436±57stat±23syst $\pi^+\pi^-$ atomic pairs from long-lived atom breakup in Pt foil were detected . The main contribution to the statistical error gives the background of $\pi^+\pi^-$ pairs generated in the Be target which is 40 times larger than the atomic pair number. It was discussed in chapter 6 that the magnet installation after Be target allows to increase an order of magnitude the proton beam intensity and decrease the background level by about two orders of magnitude. The statistical error significantly decreases and systematic error can be also suppressed. In this scheme the number of produced $\pi^+\pi^-$, π^+K^- and $K^+\pi^-$ atoms per time unit increases 370, 1600 and 750 times accordingly. The $\pi^+\pi^-$ atomic pair number per time unit increases less than the atom number. Nevertheless this increasing is two orders of magnitude. The large statistics and background suppression allow to use the model independent analysis for the Lamb shift and combination of $\pi\pi$ scattering length $2a_0 + a_2$ measurements. This analysis uses Lorentz transformation and quantum mechanics only.

8 Acknowledgments

We are grateful to M.Gadzitski and A.Korzenev for offering of unpublished data on inclusive cross sections for p-C interactions at P_p = 31 GeV/c. We are grateful also to V.Uzhinsky for the consulting on FTF generator.

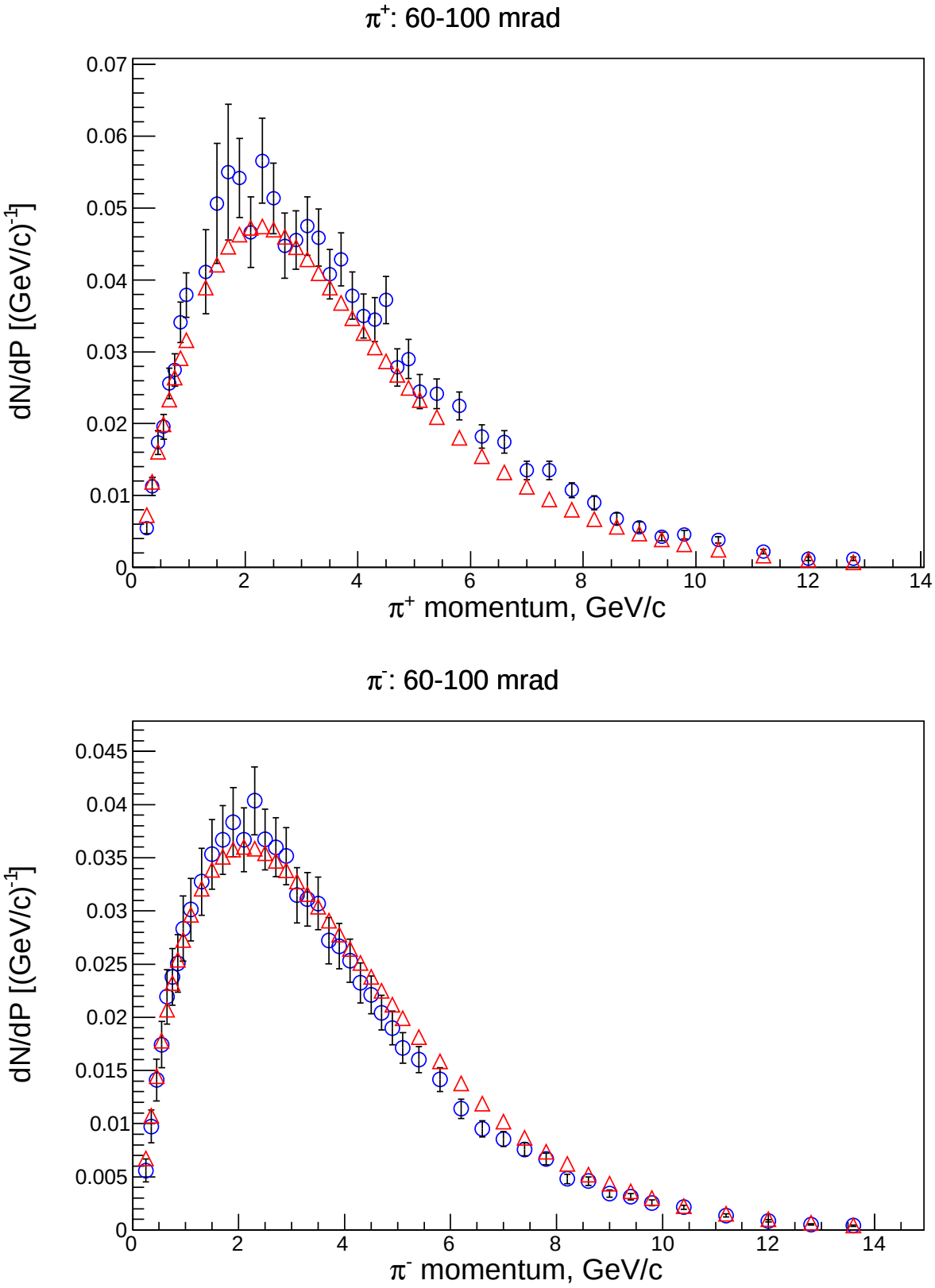

Figure 1: The yields of π^+ and π^- in p-C interactions at 31 GeV/c for polar angles of 40÷60 and 60÷100 *mrad*. ○ - experimental data [28] and △ - FTF simulation data.

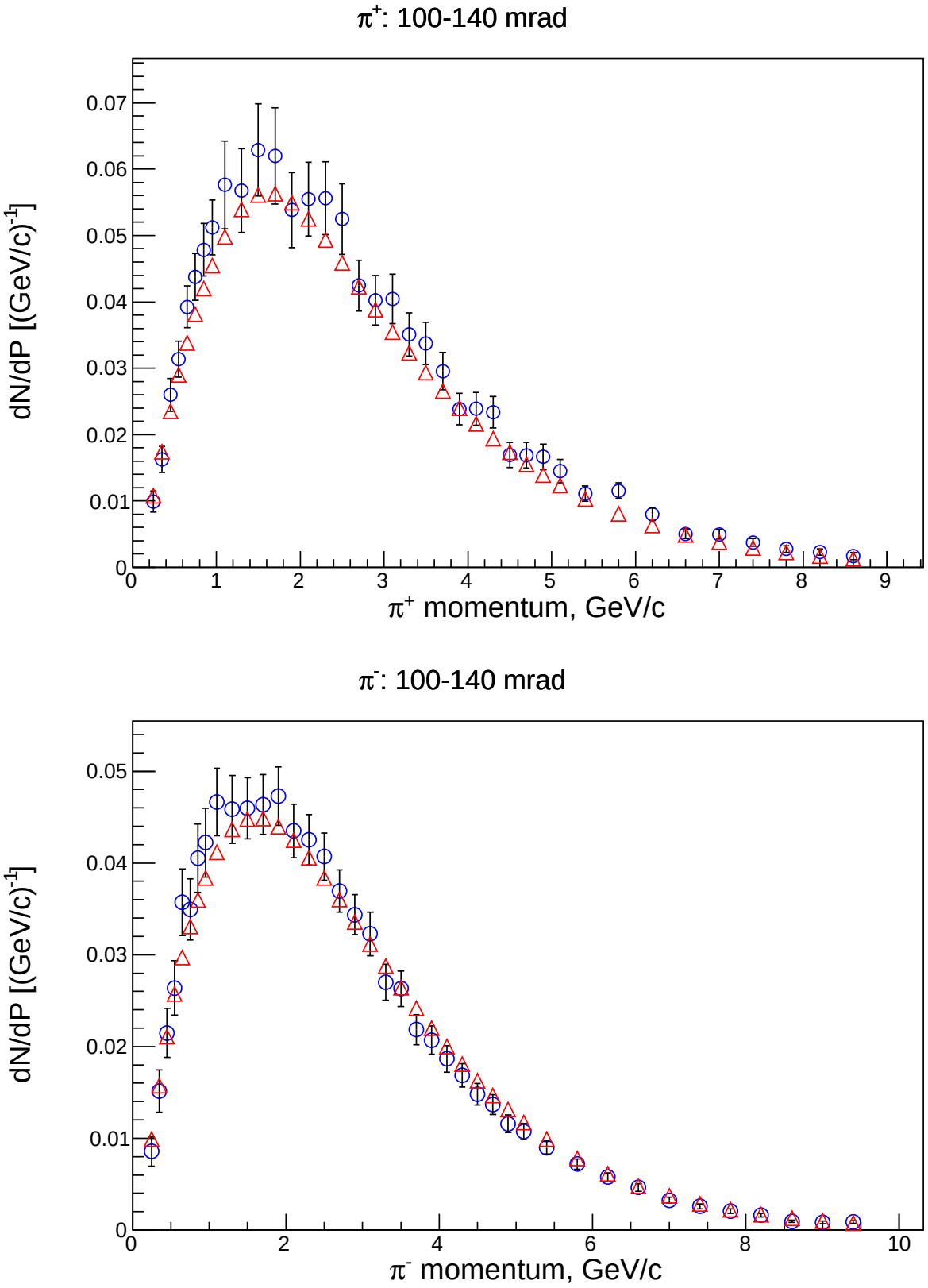

Figure 2: The yields of π^+ and π^- in p-C interactions at 31 GeV/c for polar angles of 100÷140 and 140÷180 *mrad*. ○ - experimental data [28] and △ - FTF simulation data.

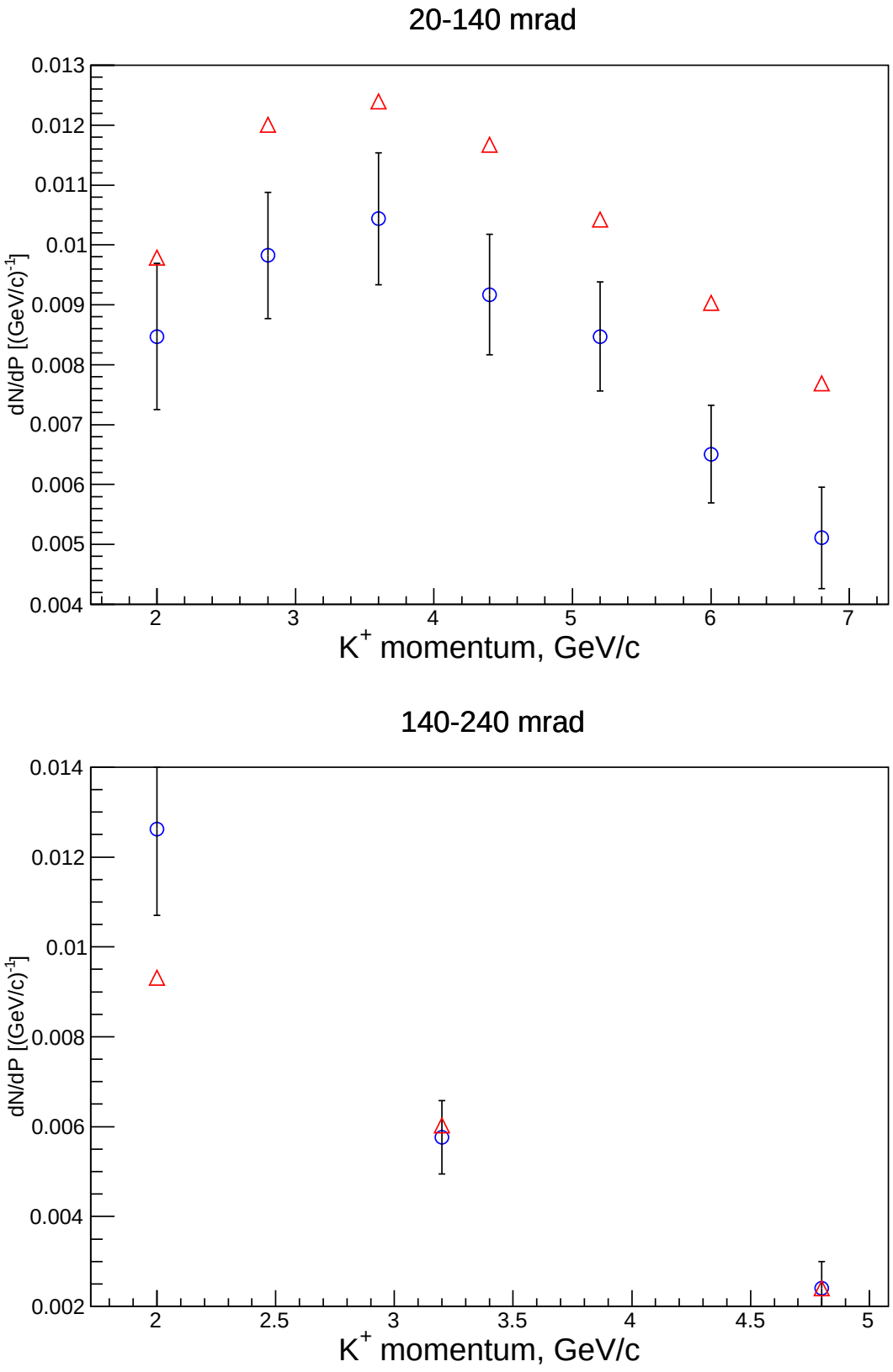

Figure 3: The yields of K^+ in p-C interactions at 31 GeV/c for polar angles of 20÷140 and 140÷240 *mrad*. ○ - experimental data [28] and △ - FTF simulation data.

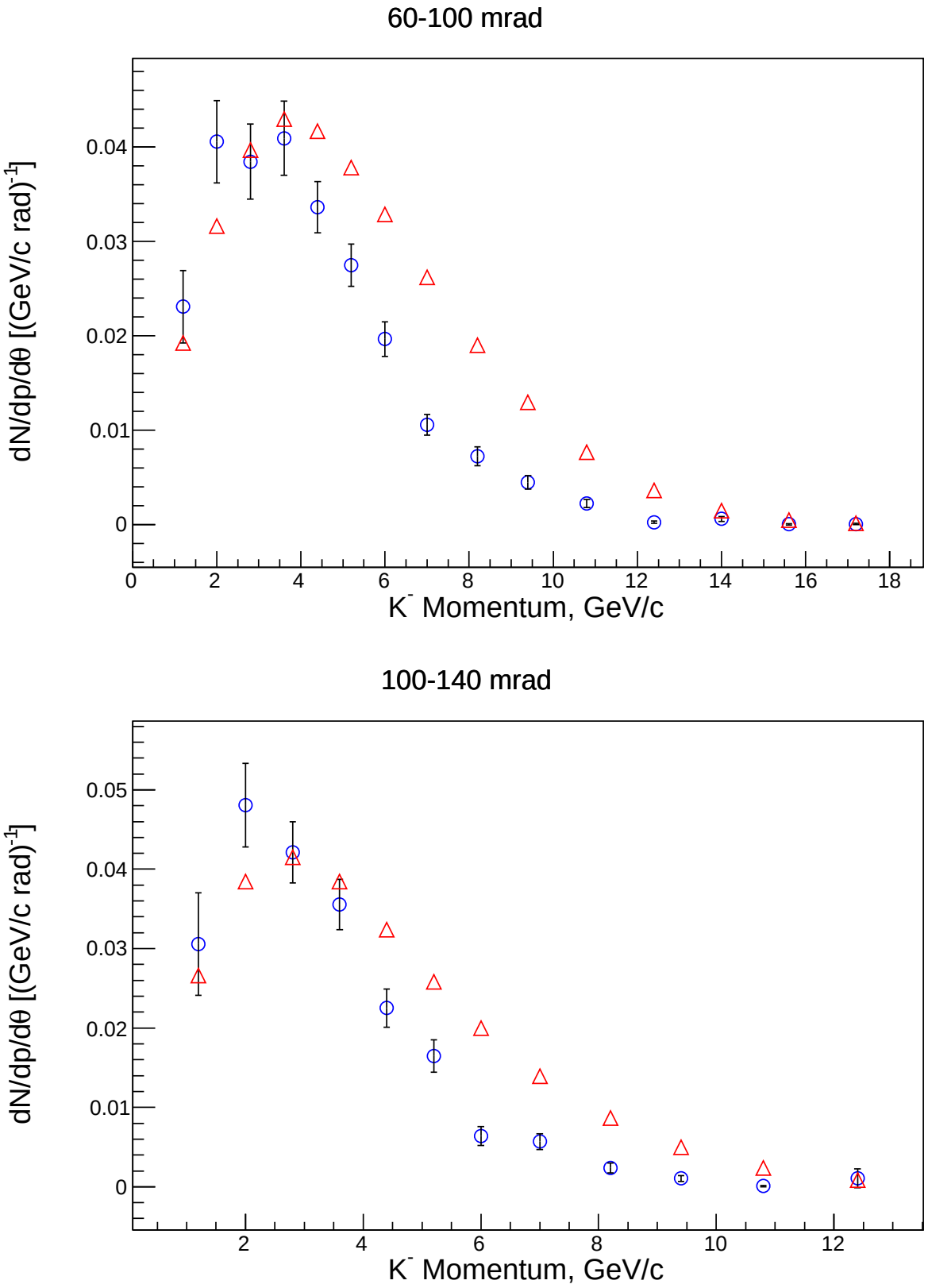

Figure 4: The yields of K^- in p-C interactions at 31 GeV/c for polar angles θ_{lab} 0÷20,20÷40,40÷60, 60÷100 and 100÷140 *mrad*. ○ - experimental data [28] and △ - FTF simulation data.

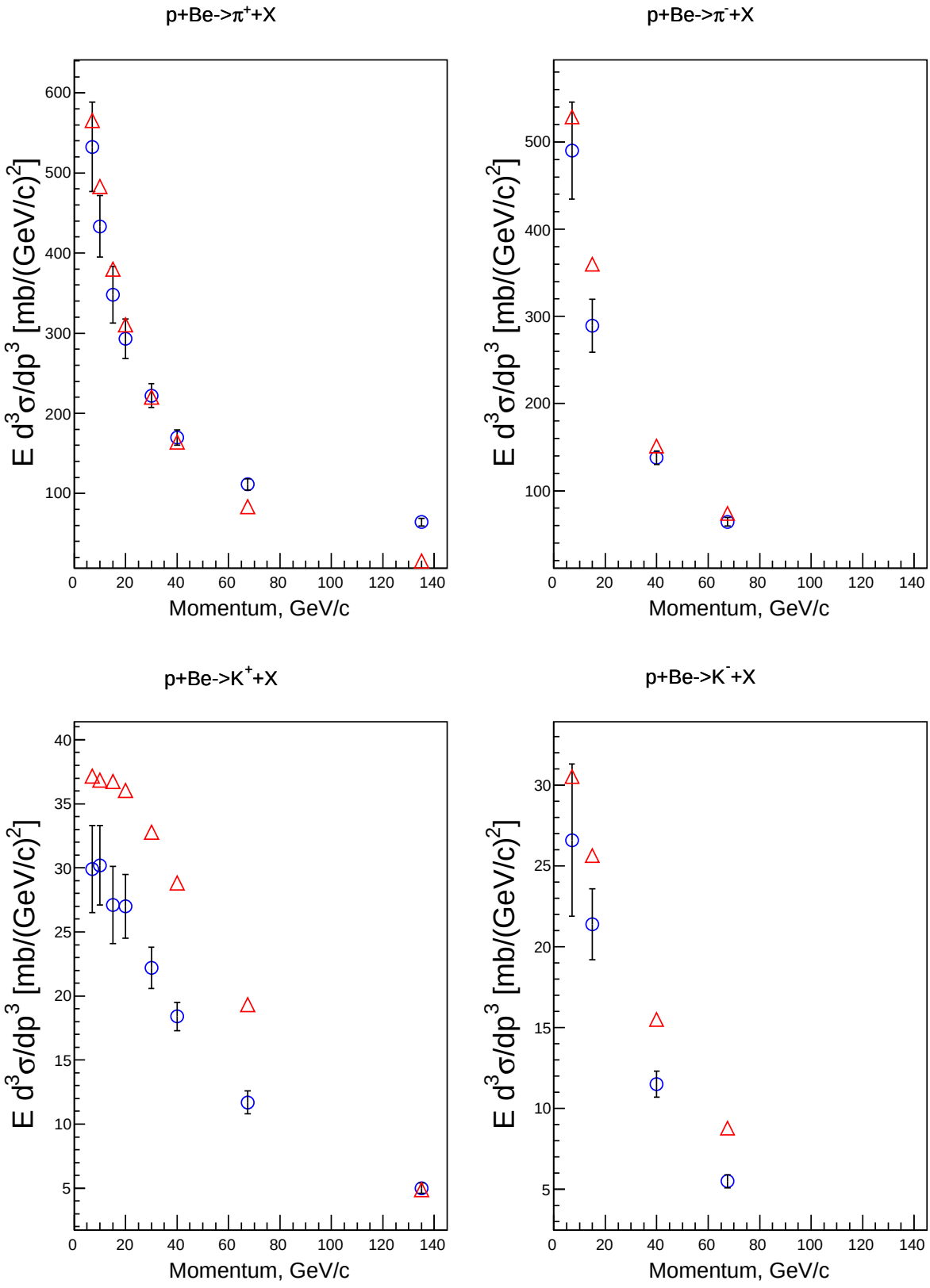

Figure 5: The invariant inclusive cross sections of π^+, π^-, K^+ and K^- in p-Be interactions at 450 GeV/c as function of particle momentum in the forward direction. ○ - experimental data [28] and △ - FTF simulation data.

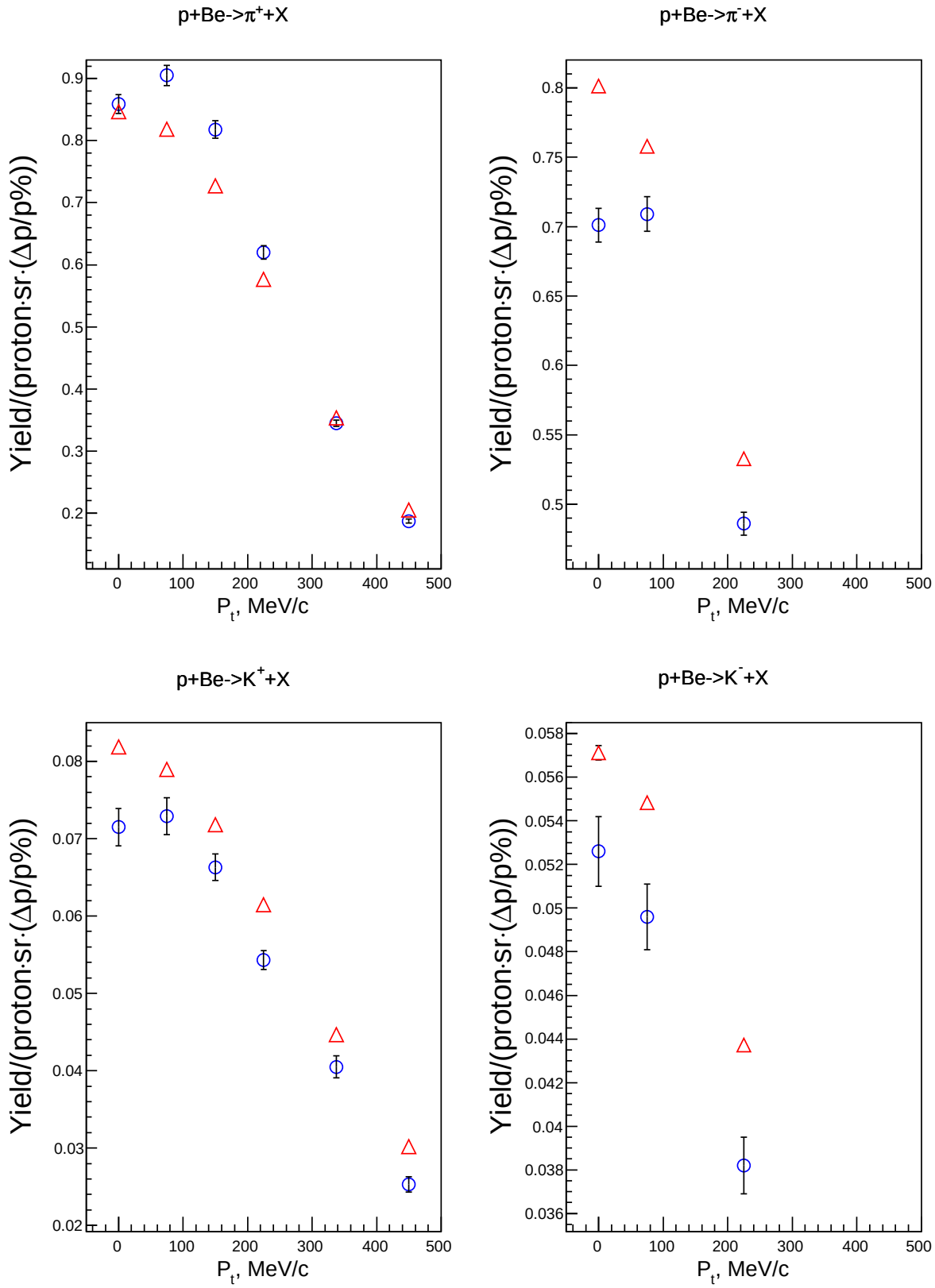

Figure 6: The yields of π^+, π^-, K^+ and K^- in p-Be interactions at 450 GeV/c as function of P_t. $\bigcirc$ - experimental data [28] and $\triangle$ - FTF simulation data.

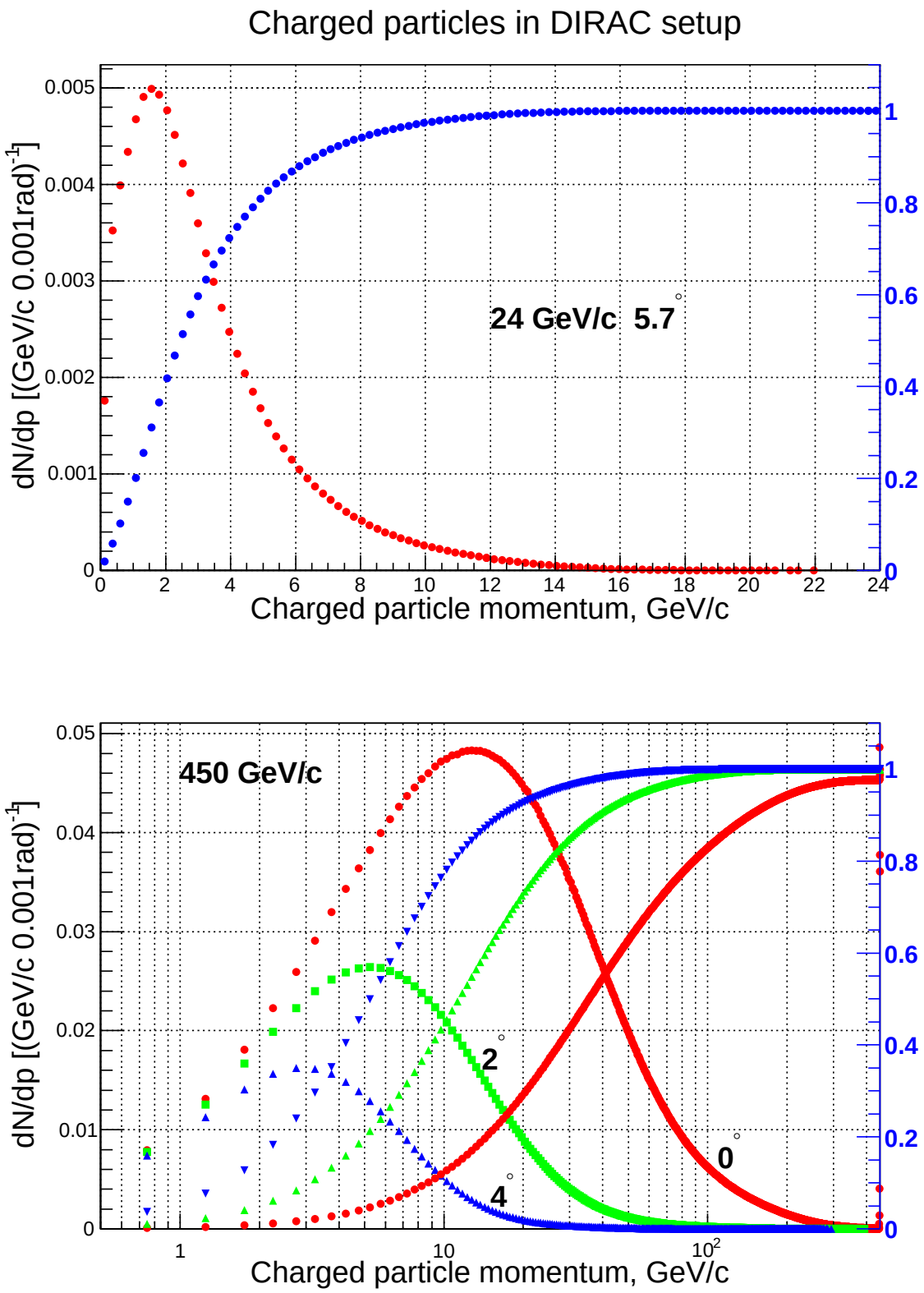

Figure 7: The total yield of charged particles ($\pi^{\pm}$, $K^{\pm}$, p and $\bar{p}$) per one p-Ni interaction at the proton momentum of 450 GeV/c and emission angles $\theta_{lab} = 0°$, $2°$, $4°$(bottom) and at the proton momentum of 24 GeV/c and emission angle $\theta_{lab} = 5.7°$(top) as a function of their momentum in l.s. for solid angle of 10^{-3} sr. Also the integrated and normalized to 1 distributions are shown.

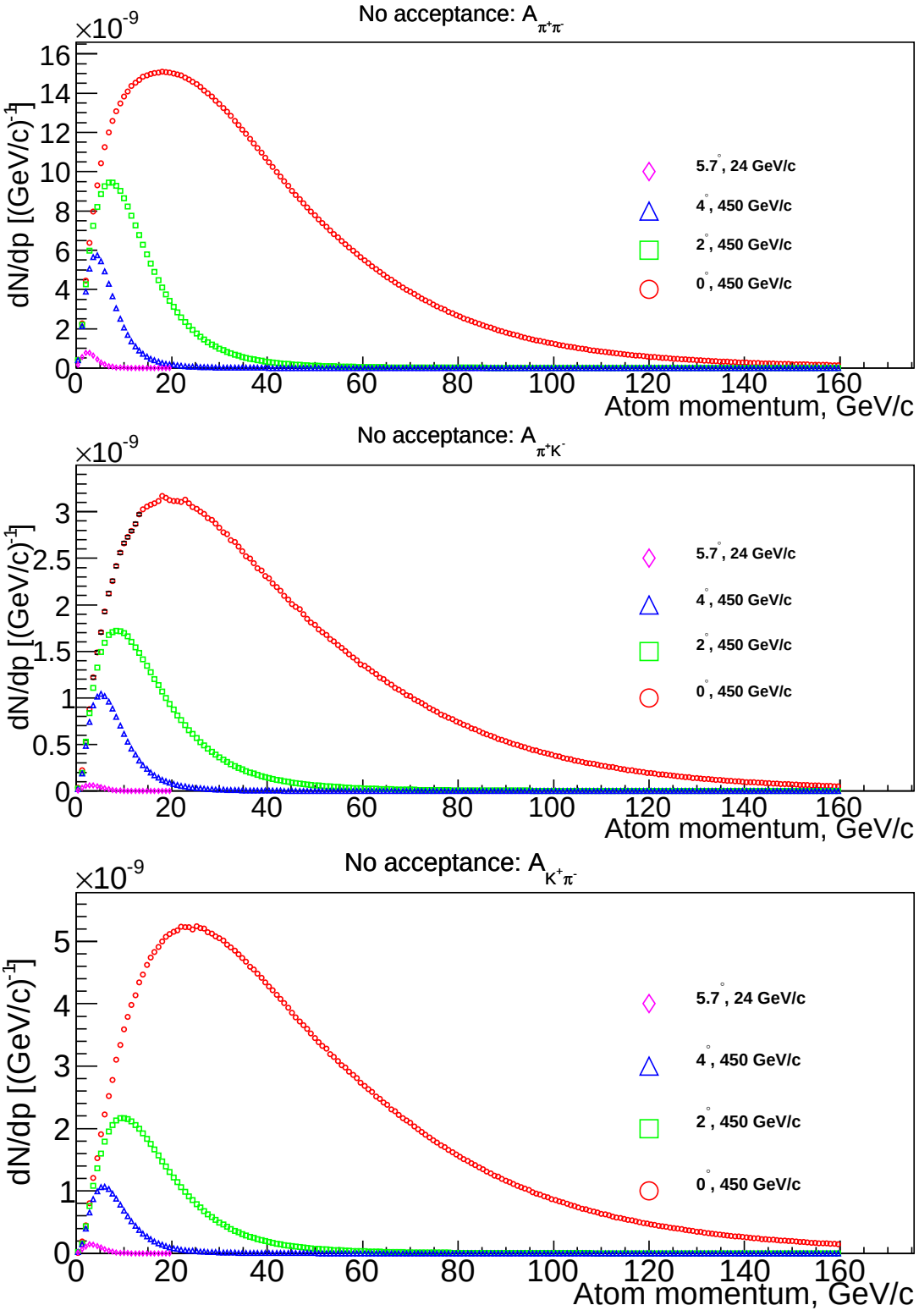

Figure 8: Yields of $A_{2\pi}$, $A_{\pi K}$ and $A_{K\pi}$ per one p-Ni interaction at the proton momentum of 450 GeV/c and emission angles $\theta_{lab} = 0°$, $2°$, $4°$ and at the proton momentum of 24 GeV/c and emission angle $\theta_{lab} = 5.7°$ as a function of the atom momentum in l.s for solid angle of 10^{-3} sr. The acceptance is not taken into account.

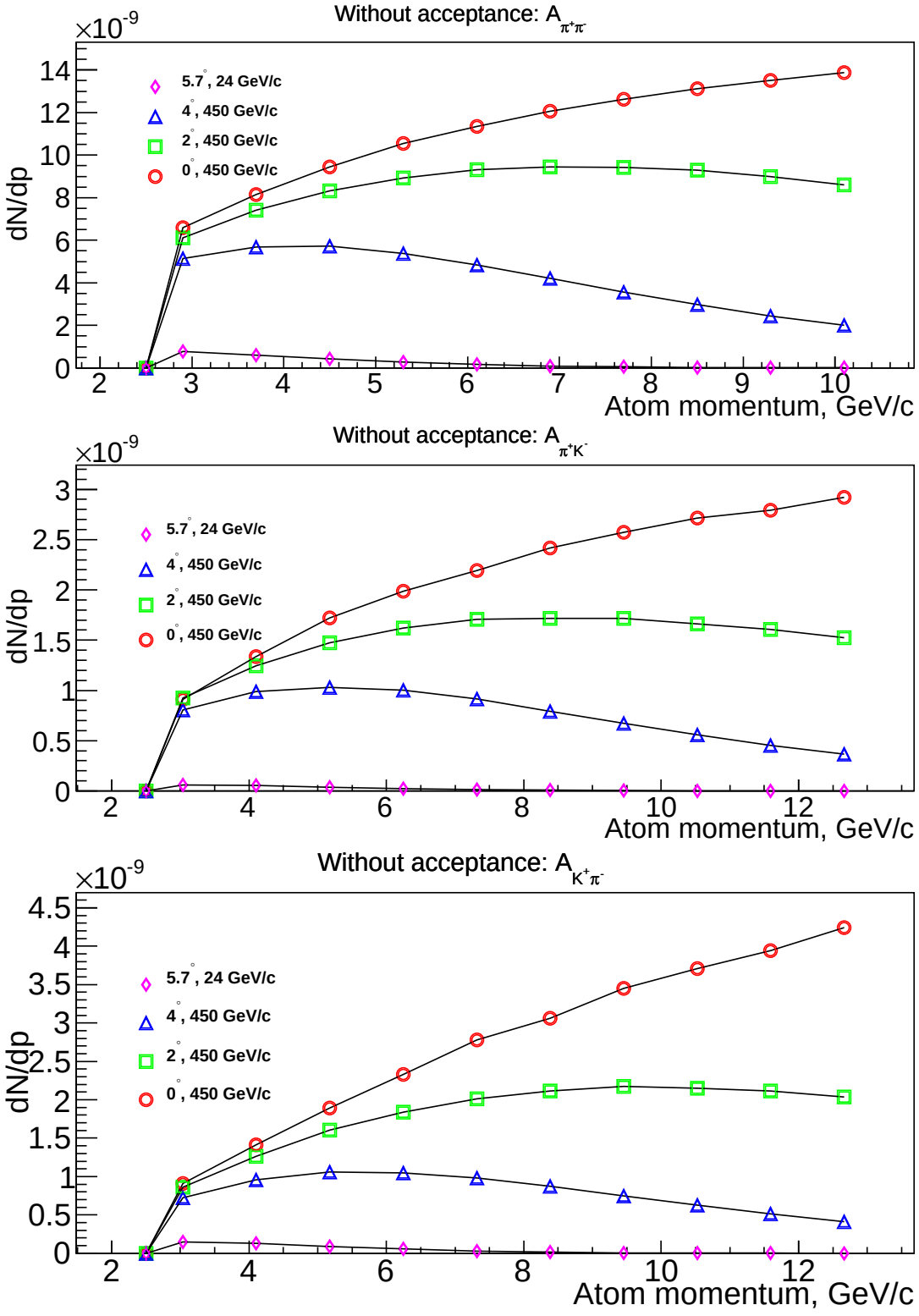

Figure 9: Yields of $A_{2\pi}$, $A_{\pi K}$ and $A_{K\pi}$ per one p-Ni interaction into solid angle of 10^{-3} sr at the proton momentum of 450 GeV/c and emission angles $\theta_{lab} = 0°$, $2°$, $4°$ and at the proton momentum of 24 GeV/c and emission angle $\theta_{lab} = 5.7°$ as a function of the atom momentum in l.s. and in the momentum interval which corresponds to the DIRAC setup. The decays are not taken into account.

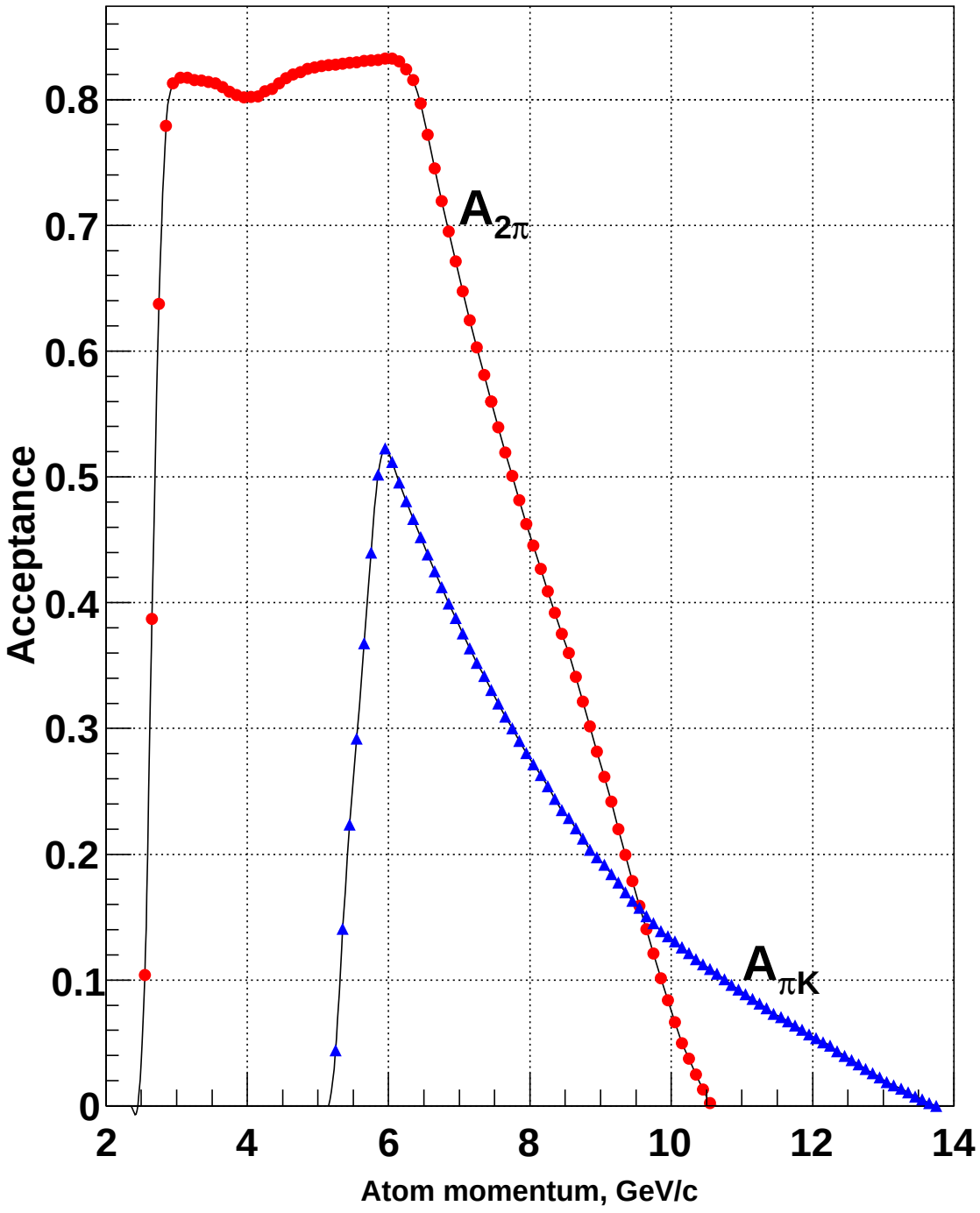

Figure 10: The acceptance behavior of the DIRAC setup for case of $A_{2\pi}$ and $A_{\pi K}$. The decays of pions and kaons are not taken into account.

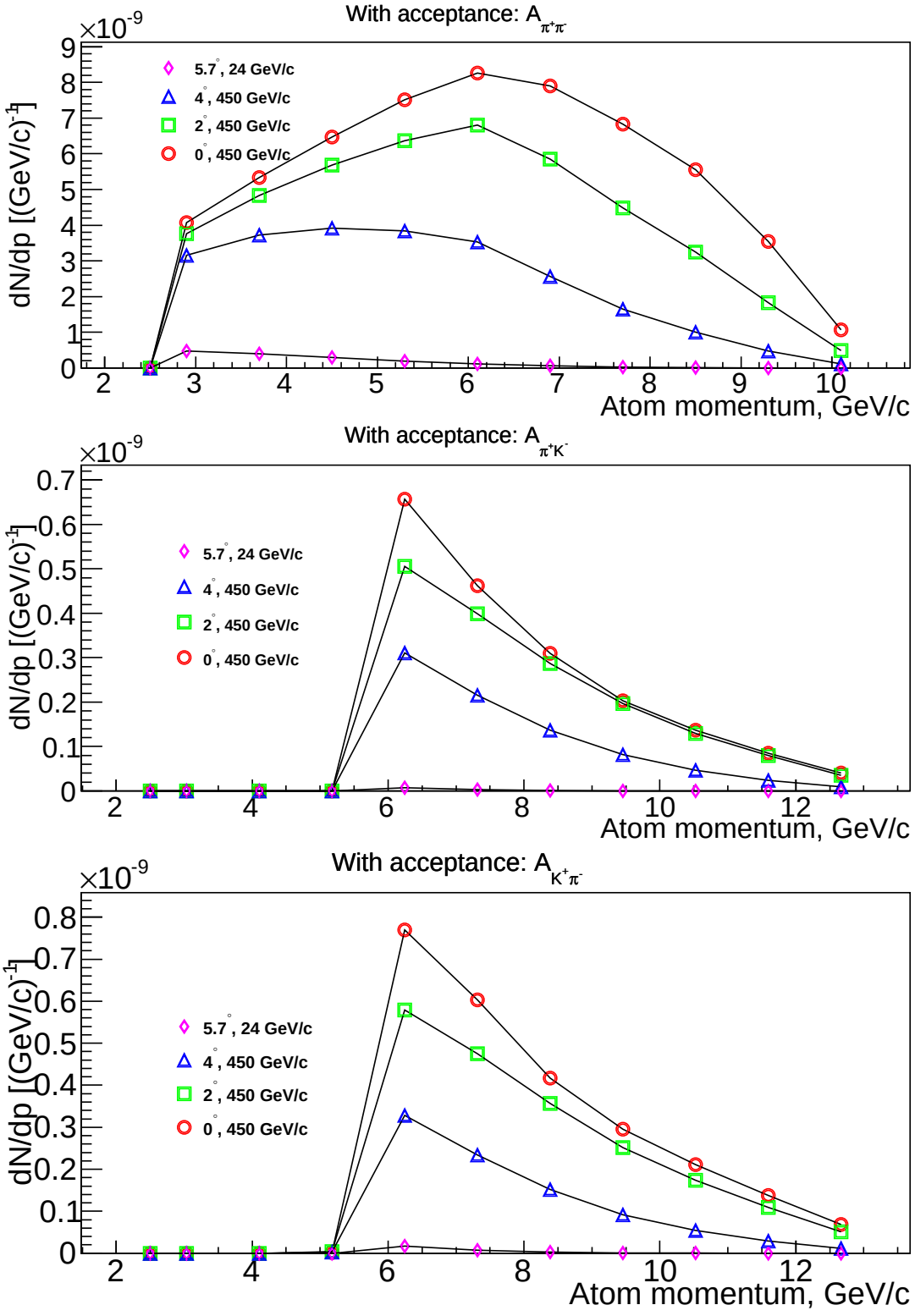

Figure 11: Yields of $A_{2\pi}$, $A_{\pi K}$ and $A_{K\pi}$ per one p-Ni interaction at the proton momentum of 450 GeV/c and emission angles $\theta_{lab} = 0°$, $2°$, $4°$ and at the proton momentum of 24 GeV/c and emission angle $\theta_{lab} = 5.7°$ as a function of the atom momentum in l.s. for solid angle of 10^{-3} sr. The acceptance of the DIRAC setup is taken into account.

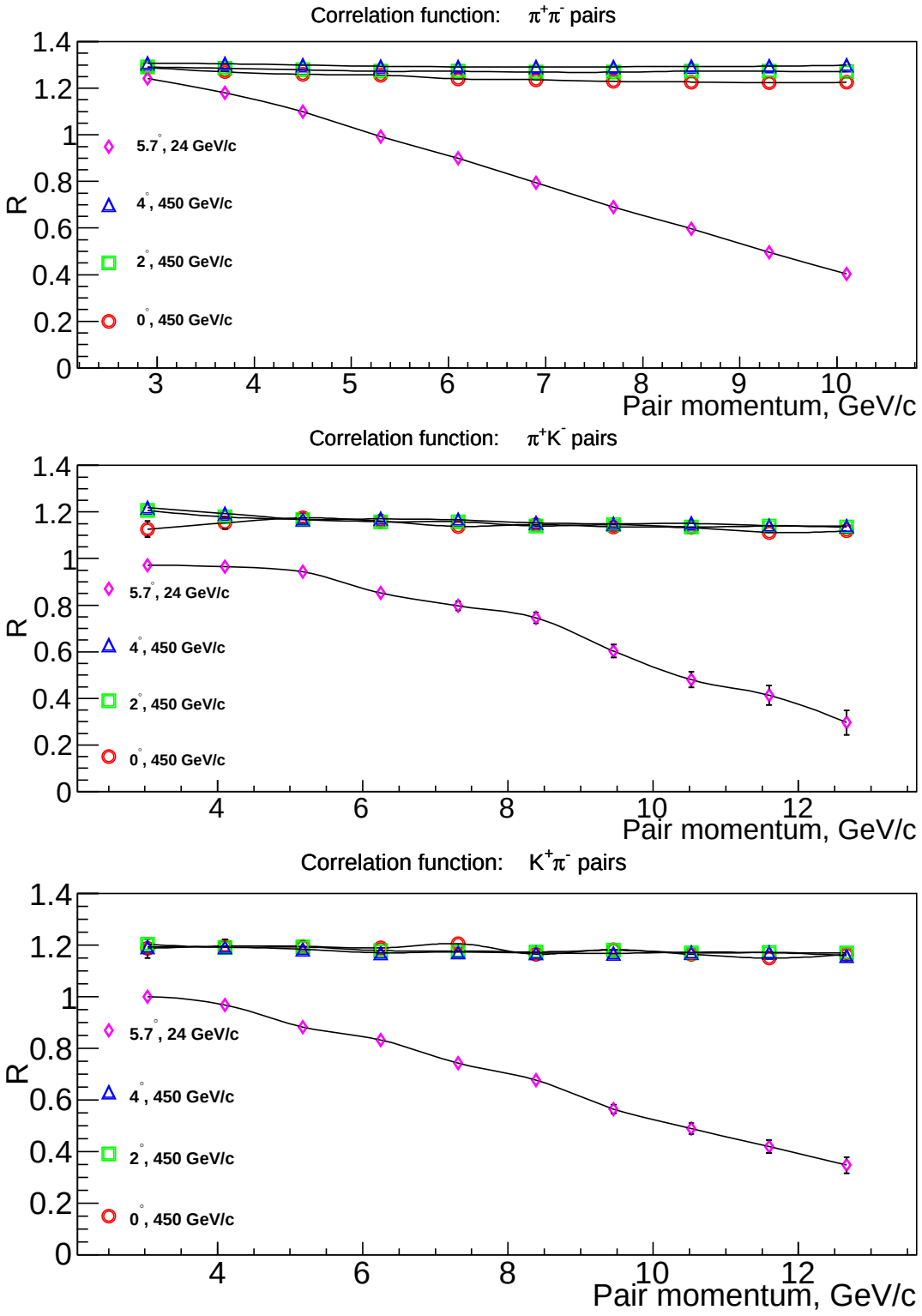

Figure 12: The dependence of correlation factor R for $\pi^+\pi^-$, π^+K^- and $K^+\pi^-$ pairs in the DIRAC setup on their momentum in l.s. for the proton momentum of 450 GeV/c and emission angles $\theta_{lab} = 0°$, $2°$, $4°$ and at the proton momentum of 24 GeV/c and emission angle $\theta_{lab} = 5.7°$.

References

[1] J.Uretsky and J.Palfrey, Phys. Rev. **121** (1961) 1798.

[2] S.M.Bilenky et al., Yad. Phys. **10** (1969) 812; (Sov. J. Nucl. Phys. **10** (1969) 469).

[3] J. Gasser et al., Phys. Rev. **D64** (2001) 016008; he*p*-ph/0103157.

[4] J.Schweizer, Phys. Lett. **B587** (2004) 33; J. Schweizer, Eur.Phys.J. C 36 (2004) 483, arXiv:hep-ph/0405034.

[5] L.G.Afanasev, at al., Phys.Lett. **B308** (1993) 200.

[6] A.Adeva et al., J. Phys. G: Nucl. Part. Phys. **30** (2004) 1929.

[7] B.Adeva at al., Phys. Lett. **B619** (2005) 50.

[8] A.Adeva et al., Phys. Lett. **B704** (2011) 24.

[9] A.Adeva et al., Phys. Lett. **B735** (2014) 288.

[10] A.Adeva et al., CERN Preprint, CERN-PH-EP-2015-175, 2015; arXiv:1508.04712;

[11] P.Buttker, S.Descotes-Genon, B.Moussallam, Eur. Phys. J. **c33** (2004) 409. J. High Energy Phys. **O405**(2004) 036 he*p*-ph/0404150 .

[12] V.Bernard et al., Nucl. Phys. **B357** (1991) 129., Phys. Rev. **D43** (1991) 3557.

[13] J.Bijnens et al., J. High Energy Phys. **O405**(2004) 036 hep-ph/0404150 .

[14] C.B.Lang, et al., Phys. Rev. **D86** (2012) 054508.

[15] L.Nemenov, Yad. Fiz. **41** (1985) 980.

[16] L.L.Nemenov and V.D.Ovsiannikov, Phys. Lett. **B514** (2001) 247.

[17] L.L.Nemenov, V.D.Ovsyannikov, E.V.Chaplygin, Nucl. Phys. **A710** (2002) 303.

[18] J.R.Bateley at al., Eur. Phys. J. **C64** (2009) 589.

[19] J.R.Bateley at al., Eur. Phys. J. **C70** (2010) 635.

[20] A.Adeva et al., CERN Preprint,CERN-PH-EP-2015-147, 2015;

[21] O.E.Gorchakov et al., Yad. Fiz. **59** (1996) 2015;(Phys. At. Nucl. **59** (1996) 1942).

[22] O.E.Gorchakov et al., Yad. Fiz. **63** (2000) 1936;(Phys. At. Nucl. **63** (2000) 1847).

[23] O.Gorchakov and L.Nemenov[JINR], DIRAC Note **2012-6**.

[24] Sjöstrand T., Bengtsson M., Com. Phys. Comm. **43** (1987) 367.

[25] V.Uzhinsky, arXiv:1109.6768[hep-ph], 2011.

[26] S. Agostinelli et al., NIMPA **506** (2003) 250.

[27] O.Gorchakov and L.Nemenov[JINR], DIRAC Note **2015-3**.

[28] N.Abgrall at al , Phys.Rev C84 034604(2011), Phys.Rev. **C85** 035210(2012), Private communication.

[29] G.Ambrosini at al.,Eur.Phys.J. **C10** (1999) 605.

[30] D.S.Barton at al.,Phys. Rev. **D27** (1983) 2580.

[31] Grishin V.G., Inclusive processes in hadron interactions at high energy. Energoizdat, Moscow 1982, p. 131 (in Russian).

[32] Eichten T. et al., Nucl. Phys. **B44** (1972) 333.

[33] A.Adeva et al., CERN Preprint, CERN-PH-EP-2015-175, 3315.

[34] S.H. Aronson et al., Phys.Rev.Lett. 48 (1982) 1078-1081.

[35] G.V.Efimov at al.,Yad.Fiz.44(1986),460;(Sov.J.Nucl.Phys. 44 (1986) 296.

[36] A.Karimhodjaev and R.N.Faustov,Yad.Fiz.29 (1979) 463;Sov.J.NuclPhys. 29 (1979) 232.